Supplementary information for

Split-Design Approach Enhances the Therapeutic Efficacy of Ligand-Based CAR-T Cells against Multiple B-cell Malignancies

Authors: Shuhong Li[1], Licai Shi[1], Lijun Zhao[1], Qiaoru Guo[1], Jun Li[2], Ze-lin Liu[3], Zhi Guo[3], Yu J. Cao[1, 4, *]

Affiliations of Institutions:

[1]State Key Laboratory of Chemical Oncogenomics, Shenzhen Key Laboratory of Chemical Genomics, Peking University Shenzhen Graduate School, Shenzhen, Guangdong, 518055, China

[2]Fundamenta Therapeutics Co., Ltd, Suzhou, Jiangsu, 215200, China

[3]Department of Hematology, Huazhong University of Science and Technology Union Shenzhen Hospital (Nanshan Hospital, Shenzhen, Guangdong 518052, China

[4]Institute of Chemical Biology, Shenzhen Bay Laboratory, Shenzhen, 518132, China

***Corresponding author:** Yu J. Cao, State Key Laboratory of Chemical Oncogenomics, Shenzhen Key Laboratory of Chemical Genomics, Peking University Shenzhen Graduate School, Shenzhen, Guangdong, 518055, China

Tel.: +86-755-2603-3107, Fax: +86-755-2603-5334, E-mail: joshuacao@pku.edu.cn

The PDF file includes:

Supplementary Figures

Supplementary Figure 5: Construction of various CAR designs and CAR-T cell preparation.

Supplementary Figure 6: Cytotoxicity validation of APRIL- and BAFF-based split-design CAR-T cells at low E:T ratios.

Supplementary Figure 7: Changes in the CAR molecular weight of 9E10-IgG4m in the presence of different concentrations of switches.

Supplementary Figure 8: Comparison of cytotoxicity between APRIL- or BAFF-based conventional CAR-T cells and split-design CAR-T cells.

Supplementary Figure 9: Characterization of patient samples from B-cell malignancies.

Supplementary Figure 10: Comparison of cytotoxicity between APRIL- or BAFF-based conventional CAR-T cells and split-design CAR-T cells in primary patient samples.

Supplementary Figure 11: Comparison of cytokine release between APRIL- or BAFF-based conventional CAR-T cells and split-design CAR-T cells in primary patient samples.

Supplementary Figure 12: Comparison of ligand-based sCAR-T cells and FDA-approved CAR-T cells against a panel of tumor cells expressing antigens with pathology-associated density.

Supplementary Figure 13: Pharmacokinetic and tissue distribution analysis of switches in mice.

Supplementary Figure 14: *In vivo* stress test of split-design APRIL-based CAR-T cells against MM.

Supplementary Figure 15: *In vivo* stress test of split-design BAFF-based CAR-T cells against B-ALL.

Supplementary Figure 16: Monitoring of mouse body weight between split-design and conventional CAR-T cells in the MM efficacy model.

Supplementary Figure 17: *In vivo* efficacy of split-design BAFF-based CAR-T cells against NHL.

Supplementary Figure 18: Validation of Nalm6 antigen escape variants.

Supplementary Figure 19: Overcoming immune escape *in vitro* with split-design ligand-based CAR-T cells.

Supplementary Figure 20: Monitoring of mouse body weight between split-design and conventional CAR-T cells in the B-ALL efficacy model.

Supplementary Figure 21: Monitoring of mouse body weight to compare APRIL-based sCAR-T cells and BCMA CAR-T cells in the MM efficacy model.

Supplementary Tables

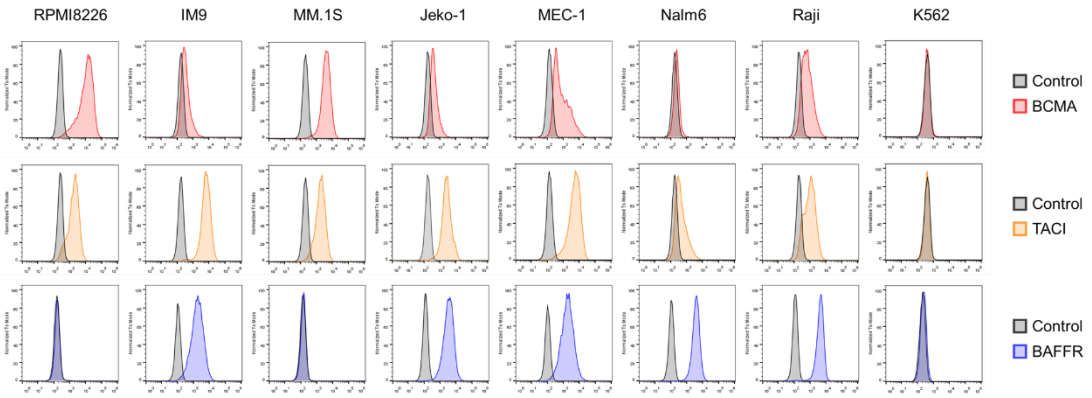

Supplementary Figure 1. Comprehensive expression of BAFFR, BCMA, and TACI antigens in B-cell malignancies.

Representative flow cytometry plots illustrating the antigens in various B-cell malignancies. Surface expression of BAFFR, BCMA and TACI antigens was evaluated using flow cytometry with APC-conjugated anti-human BAFFR antibody, PE-conjugated anti-human BCMA antibody and PE-conjugated anti-human TACI antibody. Data are representative of five independent experiments.

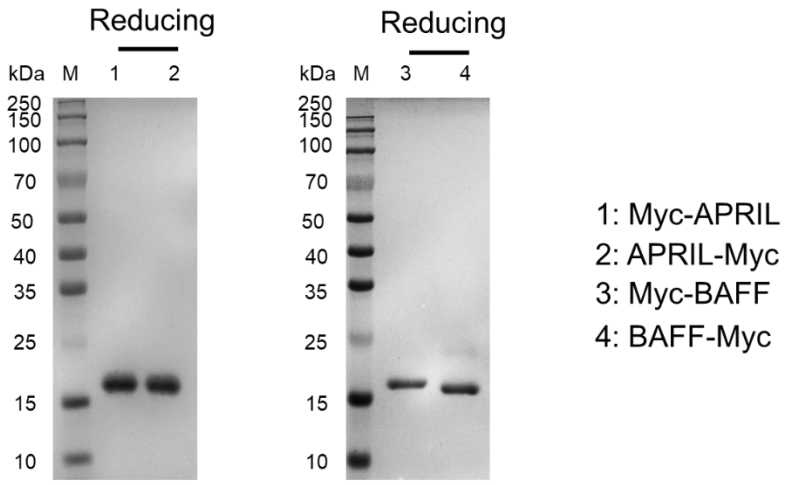

Supplementary Figure 2. Preparation and characterization of various formats of APRIL- and BAFF-based switches.

SDS–PAGE analysis of different switches under reducing conditions. Data are representative of five independent experiments.

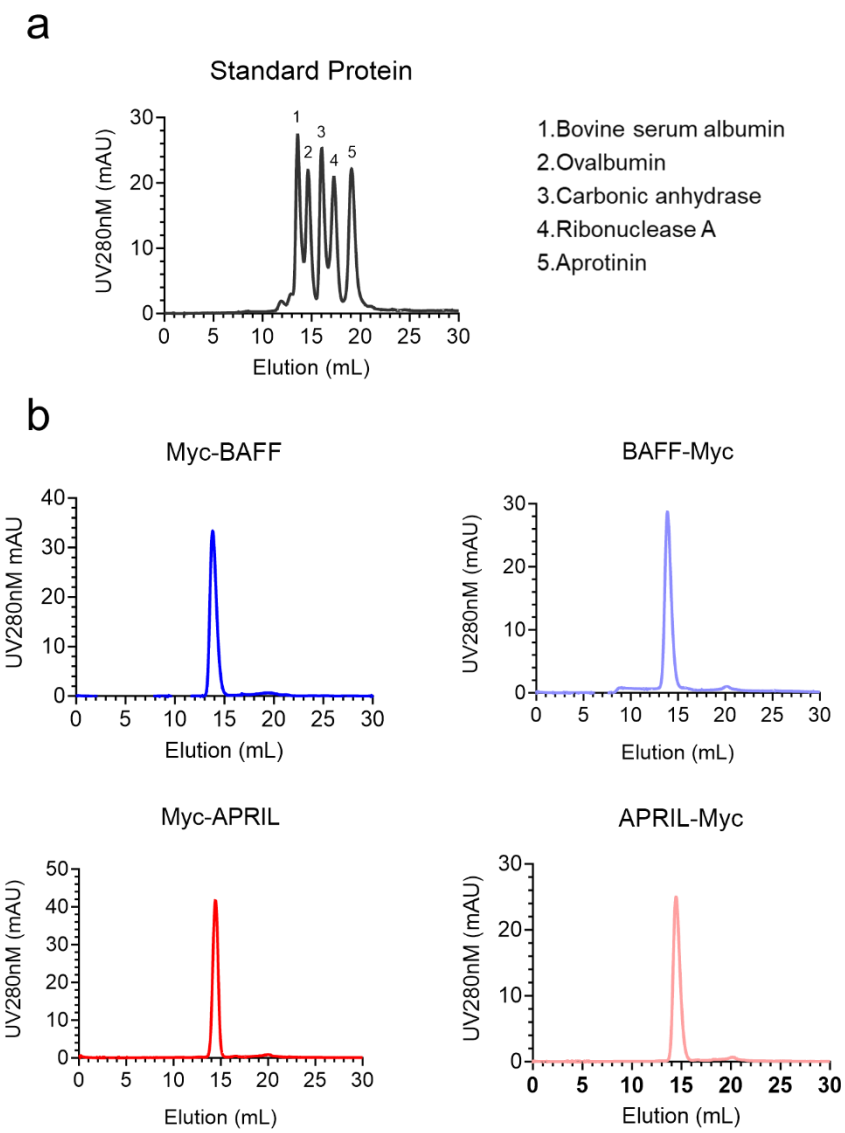

Supplementary Figure 3. Size exclusion chromatography analysis of different switches.
(a) SEC analysis of standard proteins. (b) SEC analysis of APRIL- or BAFF-based switches. Data are representative of three independent experiments. Source data are provided in the Source Data file.

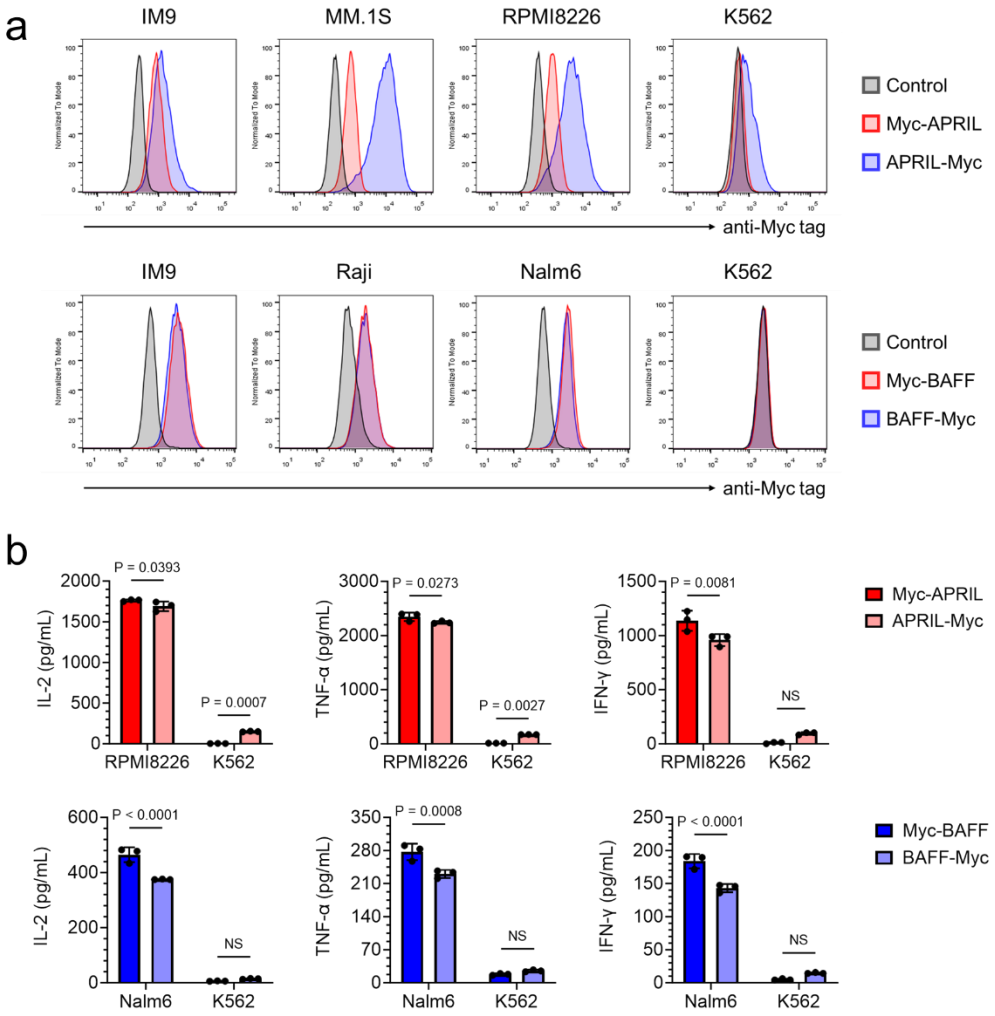

Supplementary Figure 4. Characterization of the antitumor activity of different ligand-based switch-redirected CAR-T cells

(a) Representative flow cytometry plots illustrating the binding ability of the two APRIL-based or BAFF-based switches to the indicated target cells. FITC-conjugated anti-Myc antibody was utilized as a secondary antibody for detection. (b) Comparative analysis of different switches in an inflammatory cytokine release assay. 9E10-IgG4m CAR-T cells were co-cultured with the specified target cells in the presence of 100 pM APRIL- or BAFF-based switches for 24 hours at an E:T ratio of 1:1 in triplicate. Two-way ANOVA multiple comparisons in Dunnett correction were used to assess significance. Error bars represent mean ± SD. NS indicates not significant. Data in this figure are representative of three independent experiments. Source data are provided in the Source Data file.

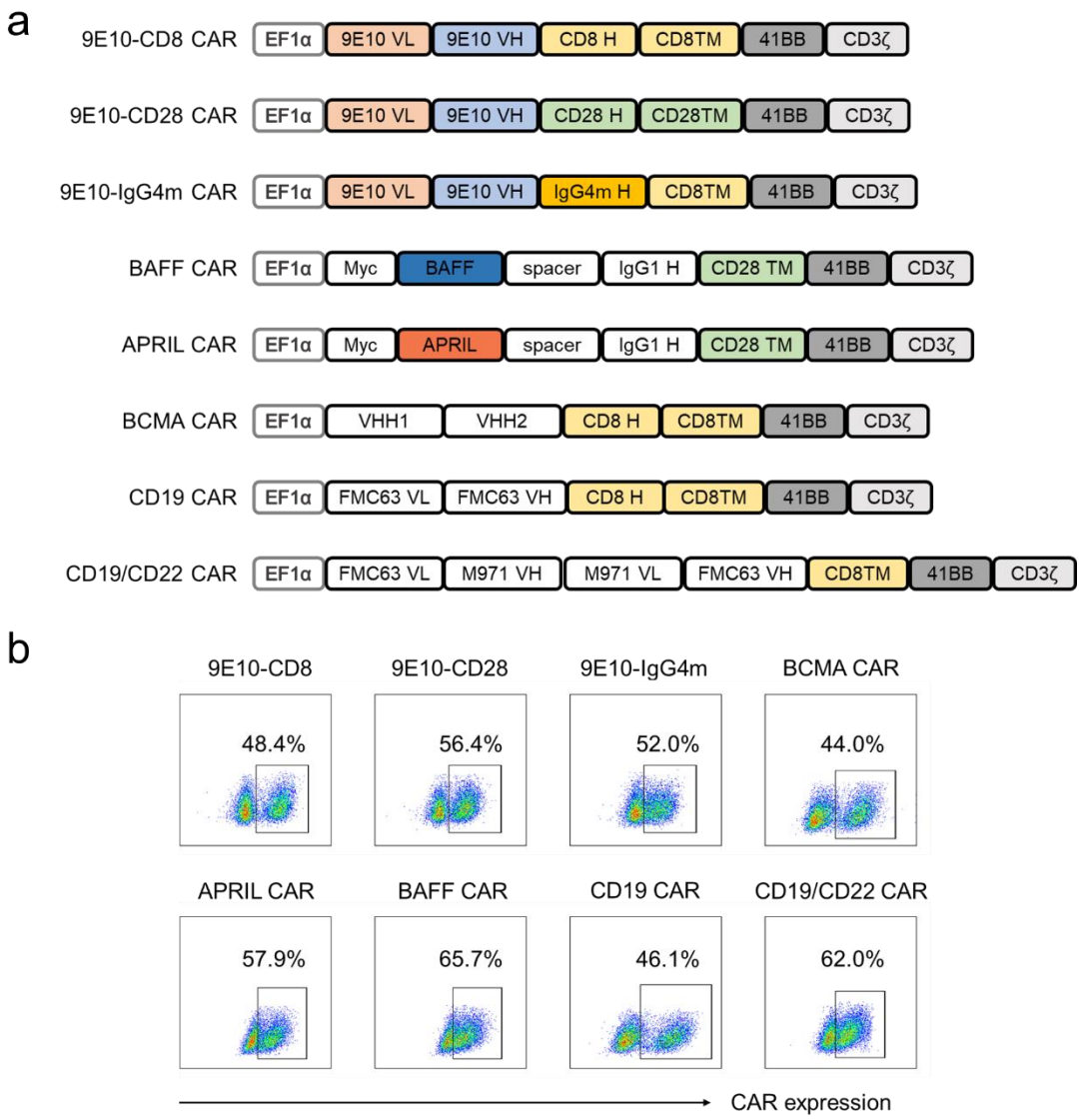

Supplementary Figure 5. Construction of various CAR designs and CAR-T cell preparation. (a) All CAR structures contain the EF1α promoter, CD8 signaling sequence, 4-1BB costimulatory domain, and CD3ζ signal transduction domain. The antigen-binding domain for the three 9E10-based CARs is the anti-Myc scFv (clone 9E10). Specifically, the 9E10-CD8 CAR employs the CD8 hinge region and transmembrane domain, the 9E10-CD28 CAR utilizes the CD28 hinge region and transmembrane domain, and the 9E10-IgG4m CAR features the IgG4m hinge region and CD8 transmembrane domain. Conventional APRIL- or BAFF-based CARs employ the extracellular domain of APRIL or BAFF as the target moiety, with a Myc tag at their N-terminus. Both utilize the IgG1 hinge region and the CD28 transmembrane domain, with a short spacer interval between the hinge region and the ligand. For the CD19 CAR, clone FMC63 targets CD19, configured as depicted in the figure, which is consistent with Tisa-cel. BCMA CAR utilized two VHH domains targeting two BCMA epitopes, as shown in the figure, which is consistent with Cilta-cel. The CD19/CD22 bispecific CAR employs clone FMC63 targeting CD19 and clone M971 targeting CD22, arranged as indicated in the figure, with a loop structure formed using flexible GGGGS linkers. (b) Representative flow cytometry plots depicting the expression of all CARs used in the study.

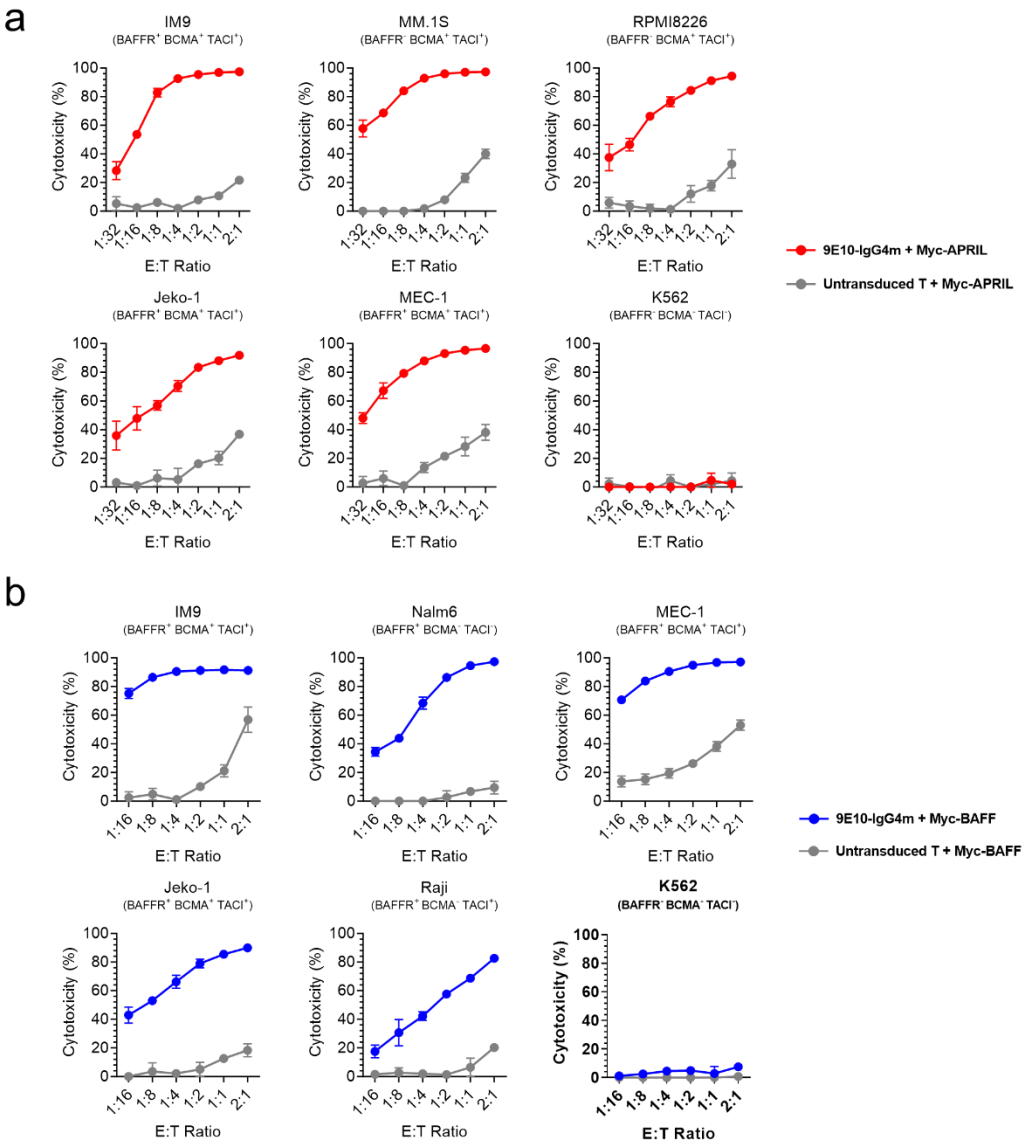

Supplementary Figure 6. Cytotoxicity validation of APRIL- and BAFF-based split-design CAR-T cells at low E:T ratios.

Cytotoxicity assays were conducted to assess the antitumor efficacy of APRIL- (a) or BAFF-based (b) sCAR-T cells against specific target cells at various E:T ratios for 24 hours in triplicate. Untransduced T cells served as controls. All the experiments were performed with a final concentration of 1 nM Myc-APRIL (a) or Myc-BAFF (b). Error bars represent mean ± SD. Data in this figure are representative of three independent experiments. Source data are provided in the Source Data file.

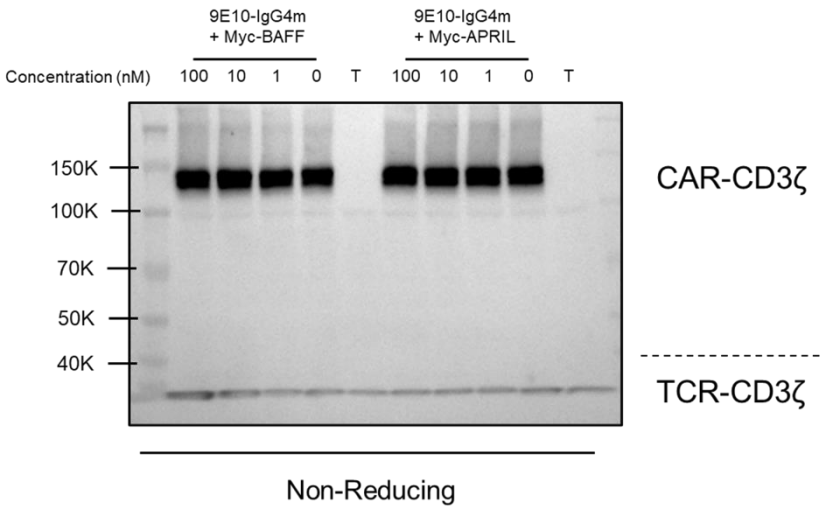

Supplementary Figure 7. Changes in the CAR molecular weight of 9E10-IgG4m in the presence of different concentrations of switches.

Western blot depicting the CAR molecular weight of 9E10-IgG4m CAR-T cells in the presence of various concentrations of switches when cultured with Nalm6 (for Myc-BAFF) or RPMI8226 (for Myc-APRIL) cells. An anti-human CD3ζ antibody was used to detect both endogenous CD3ζ and CD3ζ within the CAR signaling domain. Endogenous CD3ζ served as a control. Electrophoresis was performed under non-reducing conditions. Data are representative of three independent experiments. Source data are provided in the Source Data file.

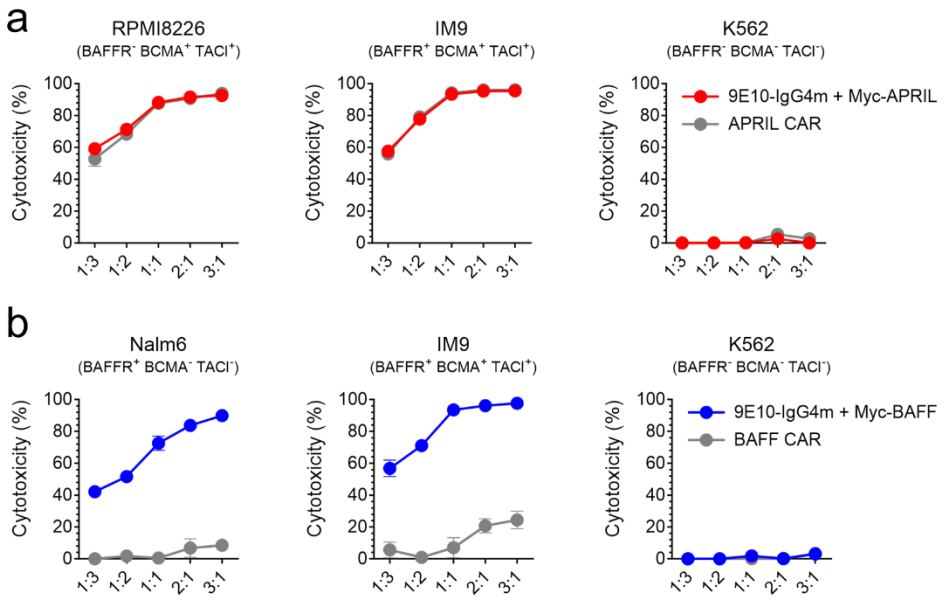

Supplementary Figure 8. Comparison of cytotoxicity between APRIL- or BAFF-based conventional CAR-T cells and split-design CAR-T cells.

Cytotoxicity assays were performed to compare APRIL- (a) or BAFF-based (b) conventional CAR-T cells and split-design CAR-T cells against indicated target cells at different E:T ratios for 24 hours in triplicate. Error bars represent mean ± SD. Data in this figure are representative of three independent experiments. Source data are provided in the Source Data file.

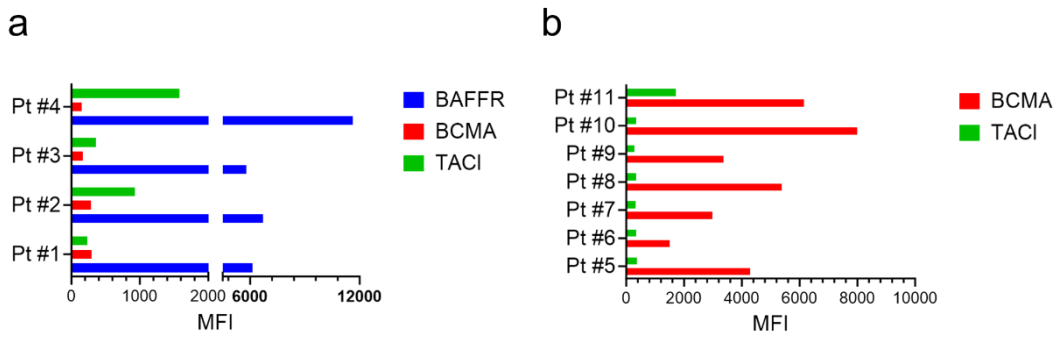

Supplementary Figure 9. Characterization of patient samples from B-cell malignancies.
(a) Quantitative analysis of BAFFR, BCMA and TACI antigen expression levels in primary patient samples from various B-cell malignancies (excluding MM) by flow cytometry. (b) Quantitative analysis of BCMA and TACI antigen expression levels in primary patient samples from MM patients by flow cytometry. Data in this figure are representative of two independent experiments. Source data are provided in the Source Data file.

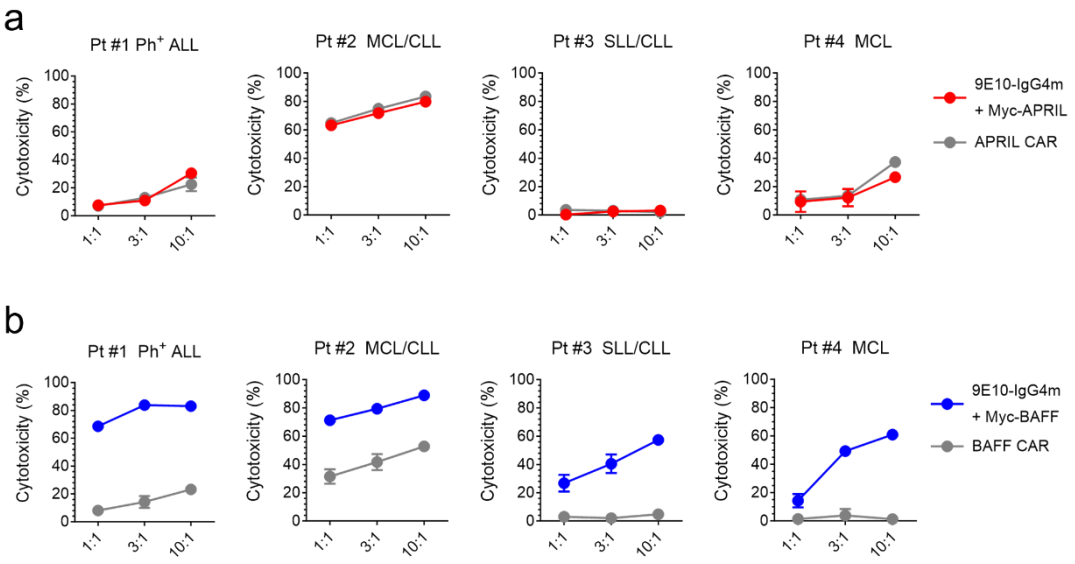

Supplementary Figure 10. Comparison of cytotoxicity between APRIL- or BAFF-based conventional CAR-T cells and split-design CAR-T cells in primary patient samples.

Cytotoxicity assays were performed using primary patient samples (Pt #1-4). APRIL- (a) or BAFF-based (b) conventional CAR-T cells and split-design CAR-T cells were co-cultured with specific primary patient tumor cells for 24 hours at various E:T ratios in triplicate. Error bars represent mean ± SD. Data in this figure are representative of three independent experiments. Source data are provided in the Source Data file.

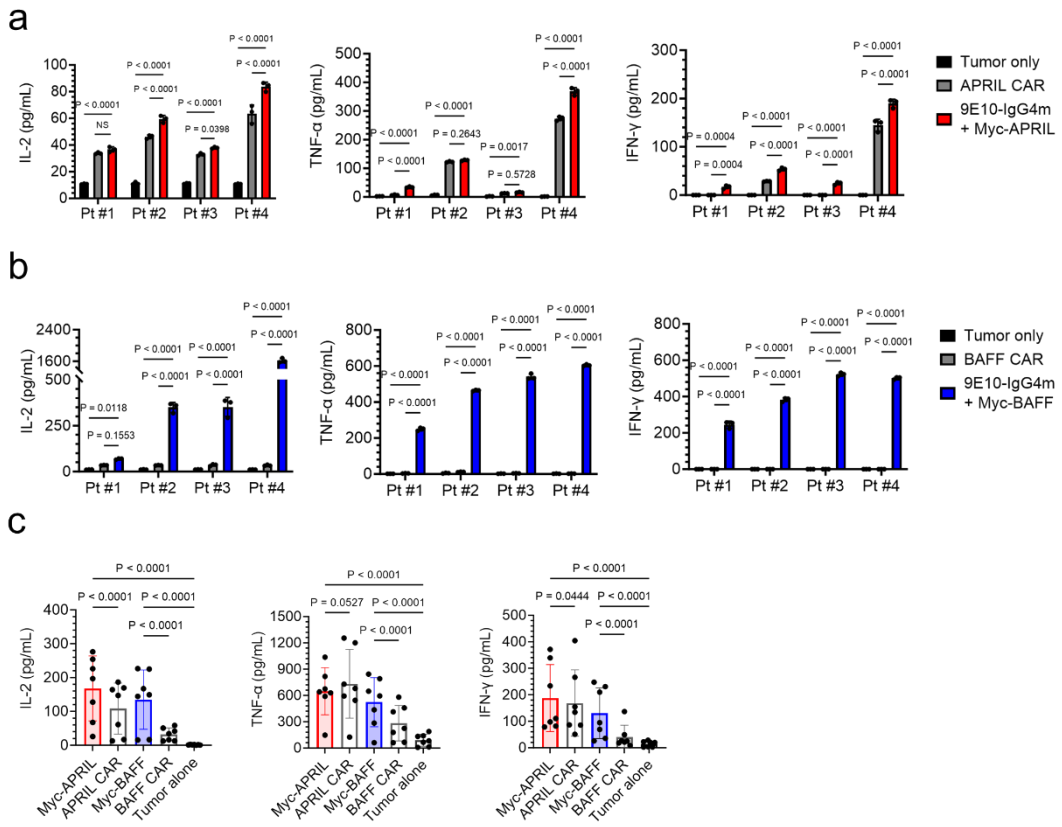

Supplementary Figure 11. Comparison of cytokine release between APRIL- or BAFF-based conventional CAR-T cells and split-design CAR-T cells in primary patient samples.

(a-b) Inflammatory cytokine release assays in primary patient samples (Pt #1-4) in triplicate. Two-way ANOVA multiple comparisons in Dunnett correction were used to assess significance. (c) Inflammatory cytokine release assay in primary MM patient samples (Pt #5-11). APRIL- or BAFF-based conventional CAR-T cells and split-design CAR-T cells were co-cultured with specific primary patient tumor cells for 24 hours at an E:T ratio of 1:1. In panel c, n = 7. All n values represent individual patient samples. One-way ANOVA multiple comparisons in Tukey correction were used to assess significance. Data are in this figure representative of three independent experiments. Error bars represent mean ± SD. NS indicates not significant. Source data are provided in the Source Data file.

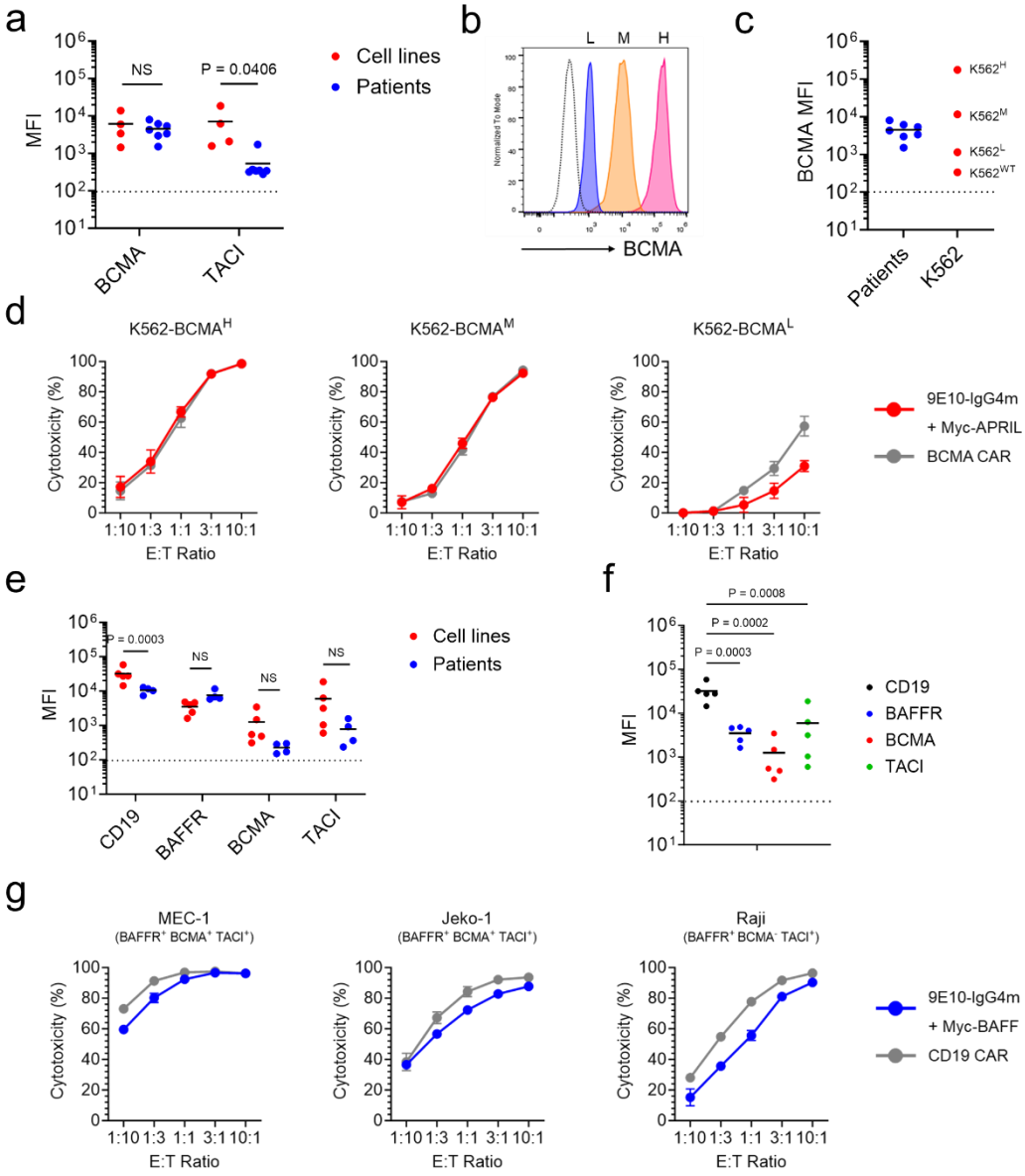

Supplementary Figure 12. Comparison of ligand-based sCAR-T cells and FDA-approved CAR-T cells against a panel of tumor cells expressing antigens with pathology-associated density.

(a) Quantitative analysis of the mean fluorescence intensity (MFI) of BCMA and TACI antigen expression in cell lines (IM9, RPMI8226, MM.1S and MEC-1) and patient-derived tumor cells (MM patients). Two-way ANOVA multiple comparisons in Dunnett correction were used to assess significance. (b) Generation of K562 cell lines transduced with variable expression levels of BCMA. The sorted cell lines were characterized as having low (L), medium (M), or high (H) expression levels. (c) MFI quantitative analysis of BCMA antigen expression in generic K562 cell lines and patient-derived tumor cells (MM patients, patients #5-11). (d) Cytotoxicity comparison of APRIL-based sCAR-T cells and BCMA CAR-T cells against different BCMA-expressing K562 variants after 24 hours of incubation at various E:T ratios in triplicate. (e) MFI quantitative analysis of CD19, BAFFR, BCMA and TACI antigen expression in cell lines (IM9, Jeko-1, MEC-1, Nalm6 and Raji) and patient-derived tumor cells (patients #1-4). Two-way ANOVA multiple comparisons in Dunnett

correction were used to assess significance. (f) Comparison of the expression levels of CD19, BAFFR, BCMA, and TACI antigens in cell lines. One-way ANOVA multiple comparisons in Dunnett correction were used to assess significance. (g) Cytotoxicity comparison of BAFF-based sCAR-T cells and CD19 CAR-T cells against different cell lines after 24 hours of incubation at various E:T ratios in triplicate. Data in this figure are representative of three independent experiments. Error bars represent mean ± SD. NS indicates not significant. Source data of (a) and (c-g) are provided in the Source Data file.

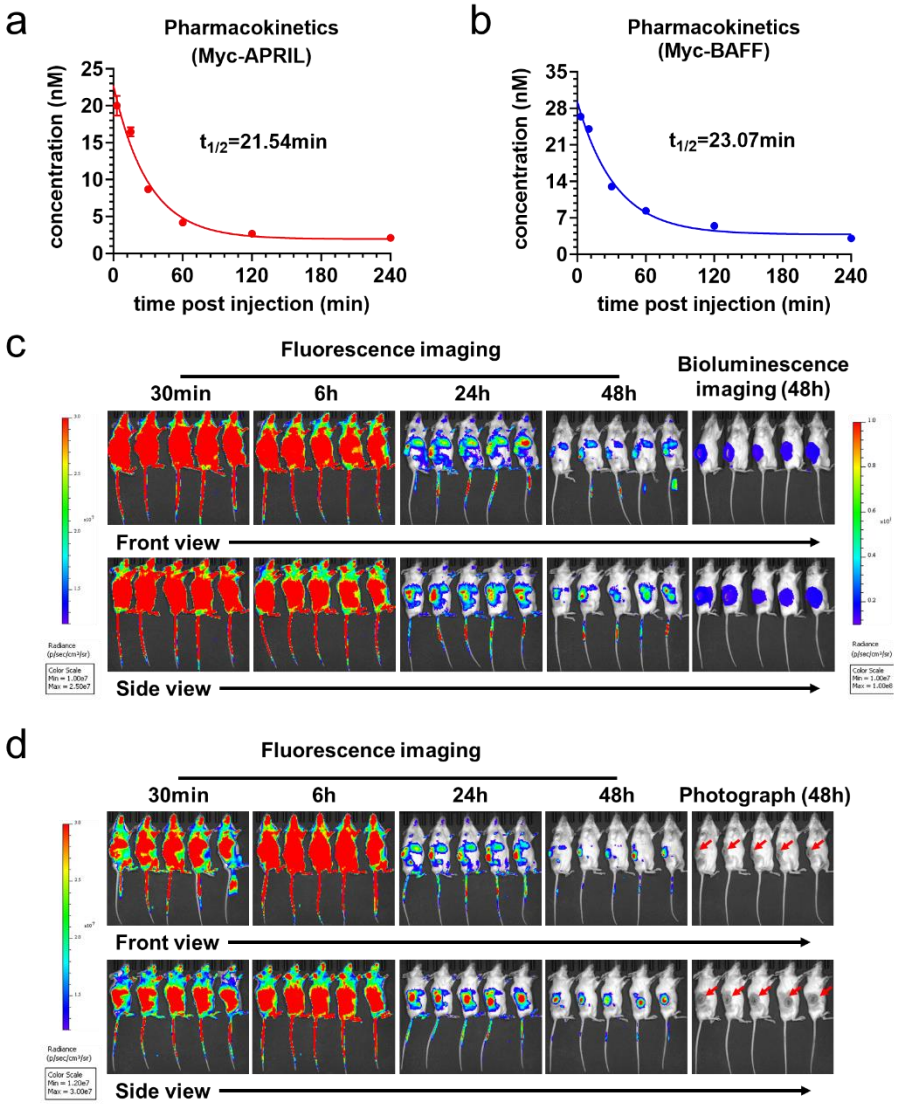

Supplementary Figure 13. Pharmacokinetic and tissue distribution analysis of switches in mice.

(a-b) Half-life of Myc-APRIL (a) and Myc BAFF (b) after i.v. administration of IRDye800-labeled switches at 3 mg/kg in female BALB/c mice (n = 3 mice/group). The concentrations of switches in peripheral blood samples were extrapolated from a standard curve. Half-life parameters were analyzed via GraphPad Prism analysis software. The mean ± SD are shown for each timepoint. (c-d) S.c. implantation of 10×10^6 RPMI8226 cells (c) or 5×10^6 Raji cells (d) in the right flank of female NSG mice (n = 5 mice/group). When the tumors reached 500 mm^3, whole-body fluorescence images of the mice were acquired by IVIS imaging at the indicated time points after i.v. administration of IRDye800-labeled switches at 3 mg/kg. For the RPMI8226 subcutaneous model, bioluminescence imaging of tumors was performed after intraperitoneal injection of D-luciferin. For the Raji subcutaneous model, arrows indicate the location of the implanted tumors. All n represents biological replicates from different mice. Data in this figure are representative of two independent experiments. Source data of (a-b) are provided in the Source Data file.

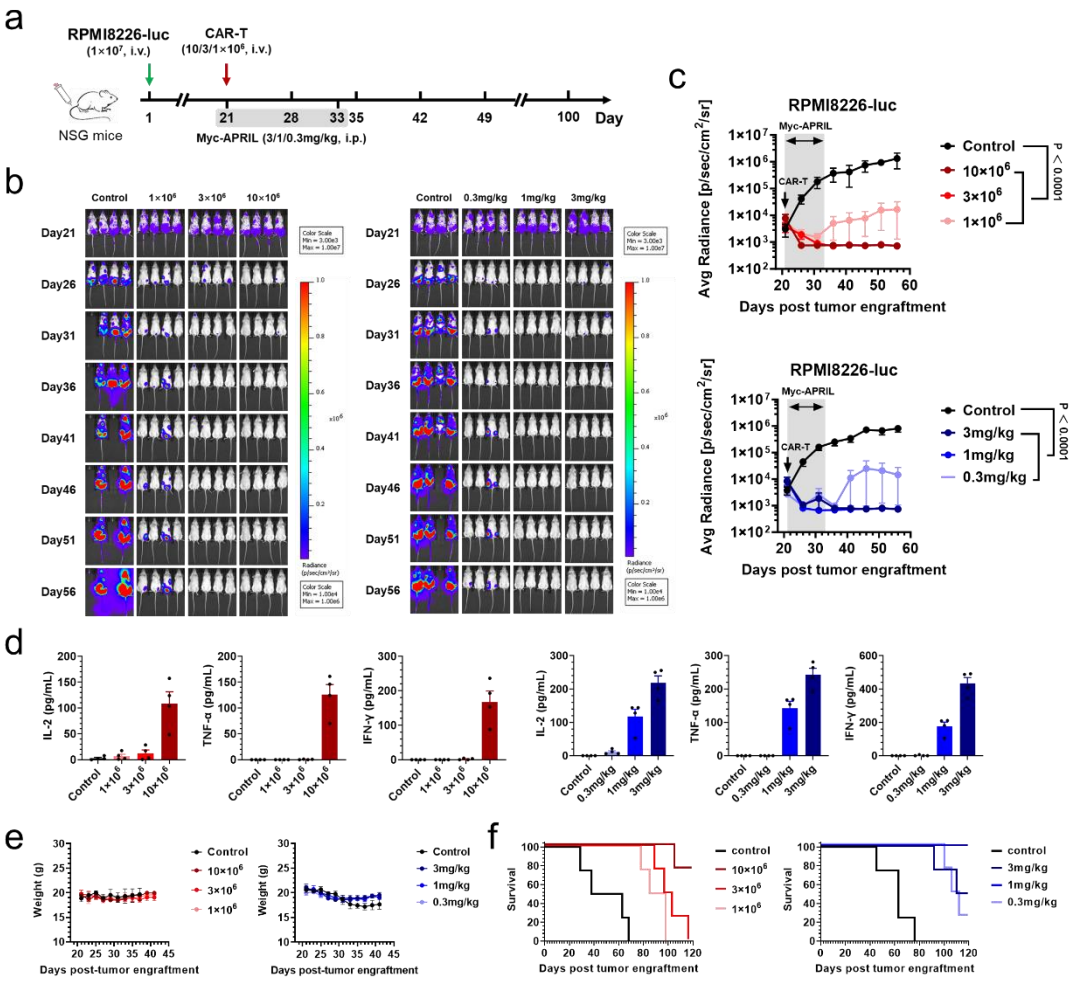

Supplementary Figure 14. ***In vivo*** **stress test of split-design APRIL-based CAR-T cells against MM.**

(a) Timeline of *in vivo* experiments. NSG mice (n = 4 mice/group) were i.v. inoculated with luciferase-expressing RPMI8226 cells (10×10^6 cells per mouse). Twenty-one days after tumor engraftment, dose–stress tests were conducted for both the CAR-T cells and the switch. For the CAR-T-cell stress test, the mice were i.v. administered 10×10^6, 3×10^6 or 1×10^6 9E10-IgG4m CAR-T cells, while the dose of Myc-APRIL was fixed at 1 mg/kg. For the switch stress test, the mice received i.p. injections of 3 mg/kg, 1 mg/kg or 0.3 mg/kg Myc-APRIL, with the CAR-T-cell dose fixed at 10×10^6. (b) Representative bioluminescence images of mice subjected to different treatments. Colors represent the luminescence intensity (red, highest; blue, lowest). (c) Quantification of the average radiance (p/s/cm2/sr) of the luminescence. Two-way ANOVA multiple comparisons in Dunnett correction were used to assess significance, comparing each 9E10-IgG4m CAR-T (with Myc-APRIL) to control group. (d) Evaluation of serum inflammatory cytokine release by ELISA 24 hours after CAR-T-cell infusion. (e) Changes in the body weights of the mice during drug administration. (f) Survival curves of mice subjected to the indicated treatments, compared using the log-rank (Mantel–Cox) test. All n represents biological replicates from different mice. Data in this figure are representative of one of two independent experiments. Error bars represent mean ± SEM. Source data are provided in the Source Data file.

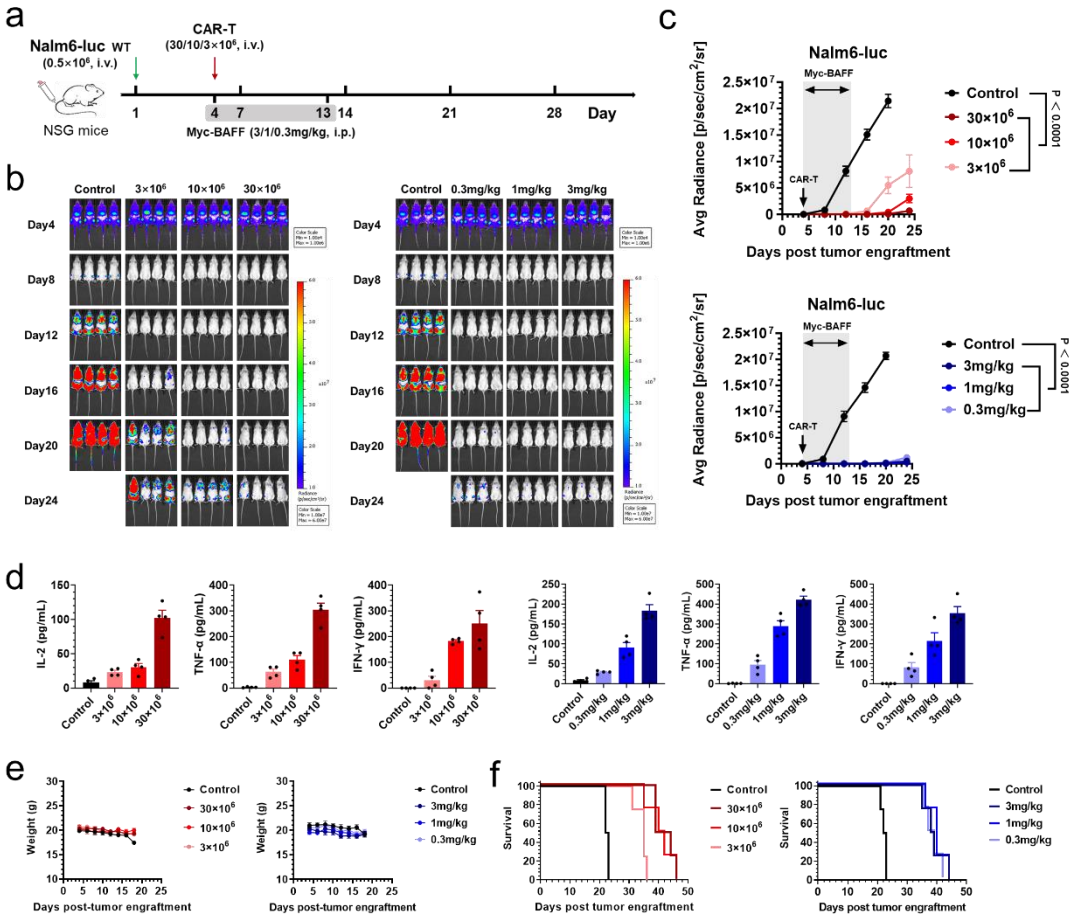

Supplementary Figure 15. *In vivo* stress test of split-design BAFF-based CAR-T cells against B-ALL.

(a) Timeline of *in vivo* experiments. NSG mice (n = 4 mice/group) received i.v. inoculation of luciferase-expressing Nalm6 cells (0.5×10^6 cells per mouse). Three days after tumor engraftment, dose–stress tests were performed for both the CAR-T cells and the switch. For the CAR-T-cell stress test, the mice were i.v. administered 30×10^6, 10×10^6 or 3×10^6 9E10-IgG4m CAR-T cells, while the dose of Myc-BAFF was fixed at 1 mg/kg. For the switch stress test, the mice received i.p. injections of 3 mg/kg, 1 mg/kg or 0.3 mg/kg Myc-BAFF, with the CAR-T-cell dose fixed at 30×10^6. (b) Representative bioluminescence images of mice subjected to different treatments. Colors represent the luminescence intensity (red, highest; blue, lowest). (c) Quantification of the average radiance (p/s/cm2/sr) of the luminescence. Two-way ANOVA multiple comparisons in Dunnett correction were used to assess significance, comparing each 9E10-IgG4m CAR-T (with Myc-BAFF) to control group. (d) Evaluation of serum inflammatory cytokine release by ELISA 24 hours after CAR-T-cell infusion. (e) Changes in the body weights of the mice during drug administration. (f) Survival curves of mice subjected to the indicated treatments, compared using the log-rank (Mantel–Cox) test. All n represents biological replicates from different mice. Data in this figure are representative of one of two independent experiments. Error bars represent mean ± SEM. Source data are provided in the Source Data file.

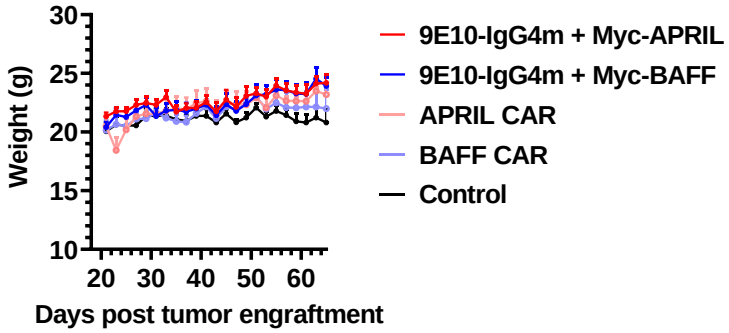

Supplementary Figure 16. Monitoring of mouse body weight between split-design and conventional CAR-T cells in the MM efficacy model.

NSG mice (n = 5 mice/group) received i.v. inoculation with luciferase-expressing RPMI8226 cells (10×10^6 cells per mouse). After the infusion of the corresponding CAR-T cells, switches were i.p. administered at a dose of 1 mg/kg every other day for a total of seven doses. Mouse body weight was monitored every other day. Error bars represent mean ± SEM. N represents biological replicates from different mice. Data are representative of one of two independent experiments. Source data are provided in the Source Data file.

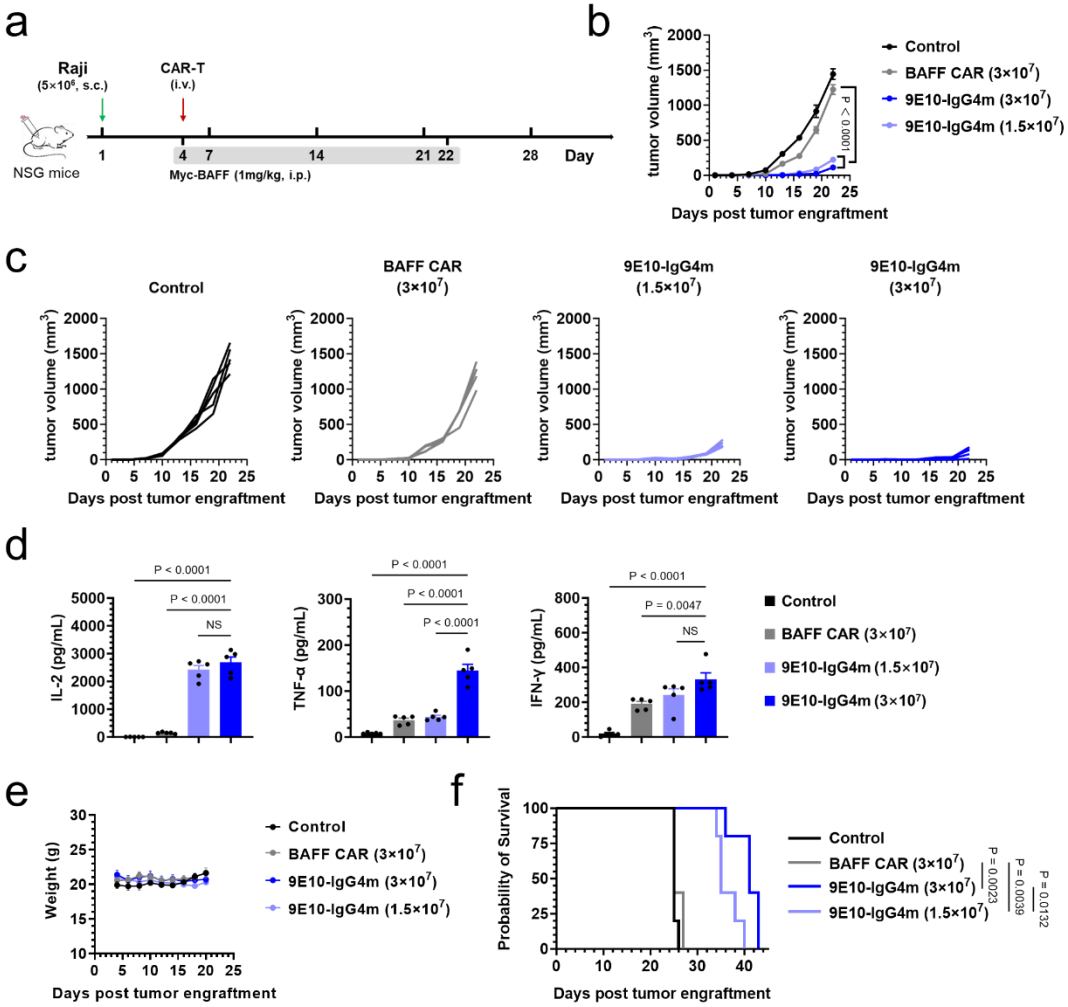

Supplementary Figure 17. *In vivo* efficacy of split-design BAFF-based CAR-T cells against NHL.

(a) Timeline of *in vivo* experiments. NSG mice (n = 5 mice/group) received s.c. inoculation of Raji cells (5×10^6 cells per mouse). Three days after tumor engraftment, the mice were i.v. administered 3×10^7 or 1.5×10^7 corresponding CAR-T cells. Switches were i.p. administered at a dose of 1 mg/kg every other day for a total of ten doses. The mice in each group were i.p. administered 100 ng of human IL-7 for 10 injections. Consistent results were observed in two independent experiments. (b-c) Tumor size was monitored over a period of 22 days. Tumor volume (mm^3) was calculated using the formula (length × $width^2$)/2. Two-way ANOVA multiple comparisons in Dunnett correction were used to assess significance, comparing 9E10-IgG4m CAR-T (with Myc-BAFF) and BAFF CAR-T. (d) Evaluation of serum inflammatory cytokine release by ELISA 24 hours after CAR-T-cell infusion. One-way ANOVA multiple comparisons in Dunnett correction were used to assess significance. (e) Changes in the body weights of the mice during drug administration. (f) Survival curves of mice subjected to the indicated treatments, compared using the log-rank (Mantel–Cox) test. All n represents biological replicates from different mice. Data in this figure are representative of one of two independent experiments. Error bars represent mean ± SEM. NS indicates not significant. Source data are provided in the Source Data file.

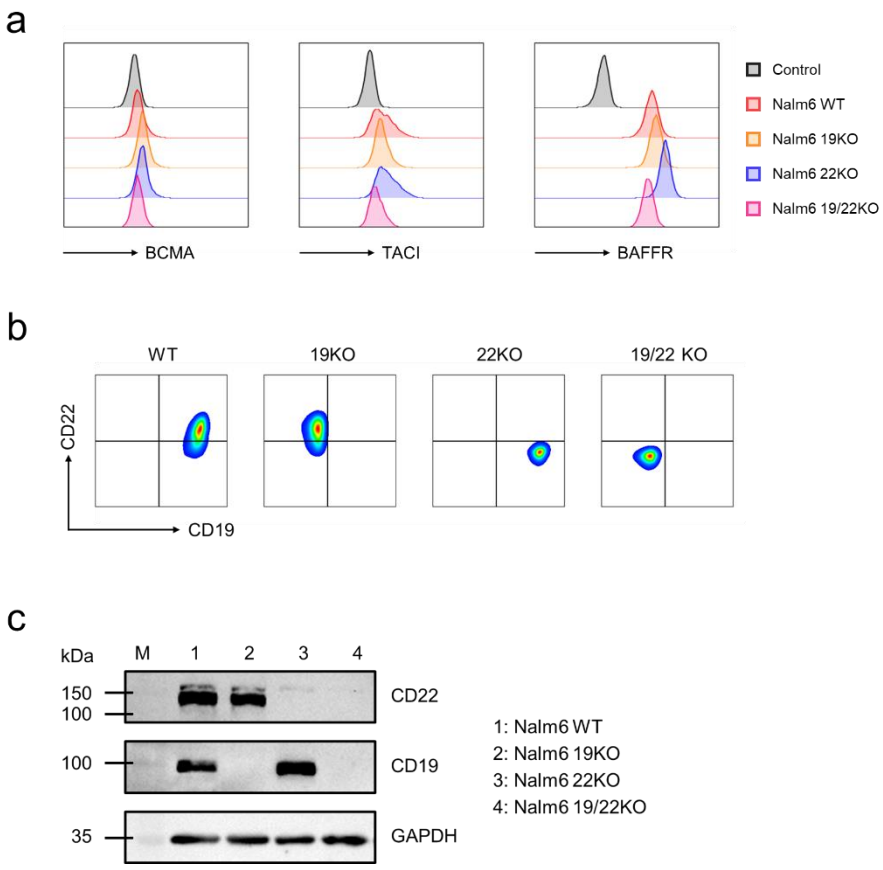

Supplementary Figure 18. Validation of Nalm6 antigen escape variants.

Nalm6 cells underwent CD19 or CD22 KO via CRISPR/Cas9. Representative flow cytometry plots illustrating cell surface antigen expression on Nalm6 antigen escape variants. (a) The surface expression of BAFFR, BCMA and TACI was analyzed by flow cytometry using APC-conjugated anti-human BAFFR antibodies, PE-conjugated anti-human BCMA antibodies and PE-conjugated anti-human TACI antibodies. (b) The surface expression of CD19 and CD22 was assessed using APC-conjugated anti-human CD19 antibody and PE-conjugated anti-human CD22 antibody. (c) Total protein from Nalm6-WT and different escape variants was collected to verify the CD19 and CD22 content by western blotting. GAPDH served as an internal reference protein. Data in this figure are representative of three independent experiments. Source data of (c) are provided in the Source Data file.

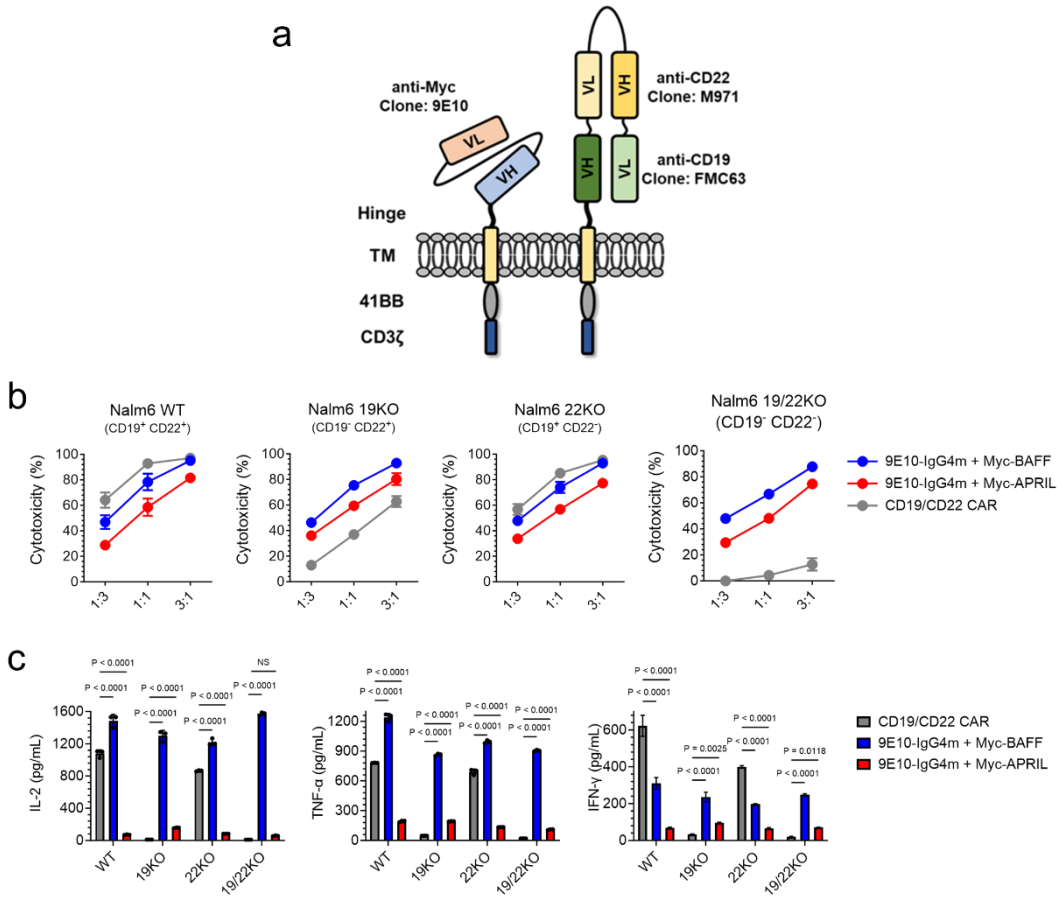

Supplementary Figure 19. Overcoming immune escape *in vitro* with split-design ligand-based CAR-T cells.

(a) Schematic structures of ligand-based sCAR and CD19/CD22 bispecific CAR structures. (b) Cytotoxicity assays of CD19/CD22 bispecific CAR-T cells and split-design CAR-T cells co-cultured with Nalm6 and the antigen escape variants at different E:T ratios for 24 hours in triplicate. (c) Inflammatory cytokine release assay. CD19/CD22 bispecific CAR-T cells and split-design CAR-T cells co-cultured with Nalm6 and the antigen escape variants for 24 hours at an E:T ratio of 1:1 in triplicate. Two-way ANOVA multiple comparisons in Dunnett correction were used to assess significance. Data in this figure are representative of three independent experiments. Error bars represent mean ± SD. NS indicates not significant. Source data are provided in the Source Data file.

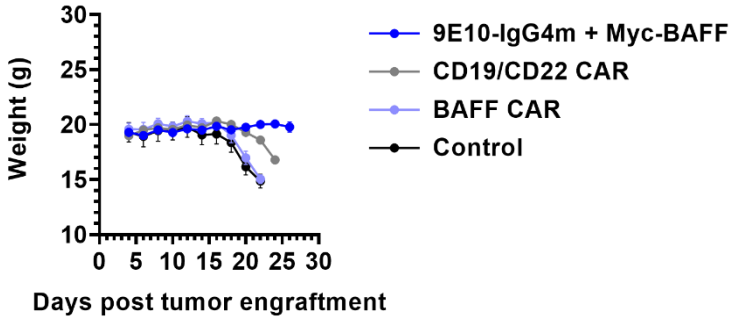

Supplementary Figure 20. Monitoring of mouse body weight between split-design and conventional CAR-T cells in the B-ALL efficacy model.

NSG mice (n = 5 mice/group) were i.v. inoculated with luciferase-expressing Nalm6 cells (1×10^6 cells per mouse). After the infusion of the corresponding CAR-T cells, switches were i.p. administered at a dose of 1 mg/kg daily for a total of ten doses. Mouse body weight was monitored every other day. Error bars represent mean ± SEM. N represents biological replicates from different mice. Data are representative of one of two independent experiments. Source data are provided in the Source Data file.

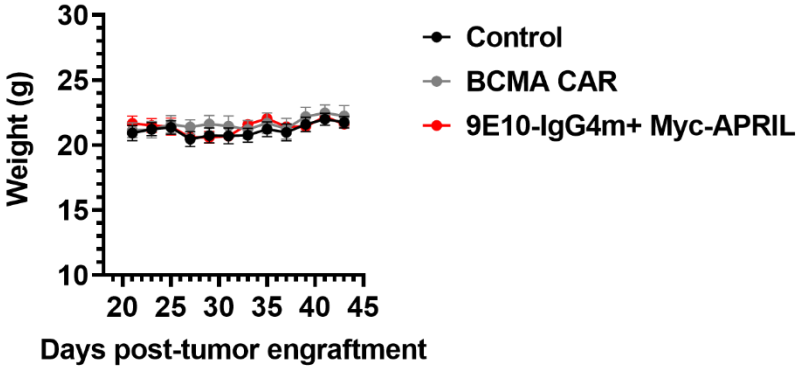

Supplementary Figure 21. Monitoring of mouse body weight to compare APRIL-based sCAR-T cells and BCMA CAR-T cells in the MM efficacy model.

NSG mice (n = 5 mice/group) received i.v. inoculation of luciferase-expressing RPMI8226 cells (10×10^6 cells per mouse). Twenty-one days after tumor engraftment, the mice were i.v. administered 10×10^6 corresponding CAR-T cells. Switches were i.p. administered at a dose of 1 mg/kg every other day, for a total of seven doses. Mouse body weight was monitored every other day. Error bars represent mean ± SEM. N represents biological replicates from different mice. Data are representative of one of two independent experiments. Source data are provided in the Source Data file.

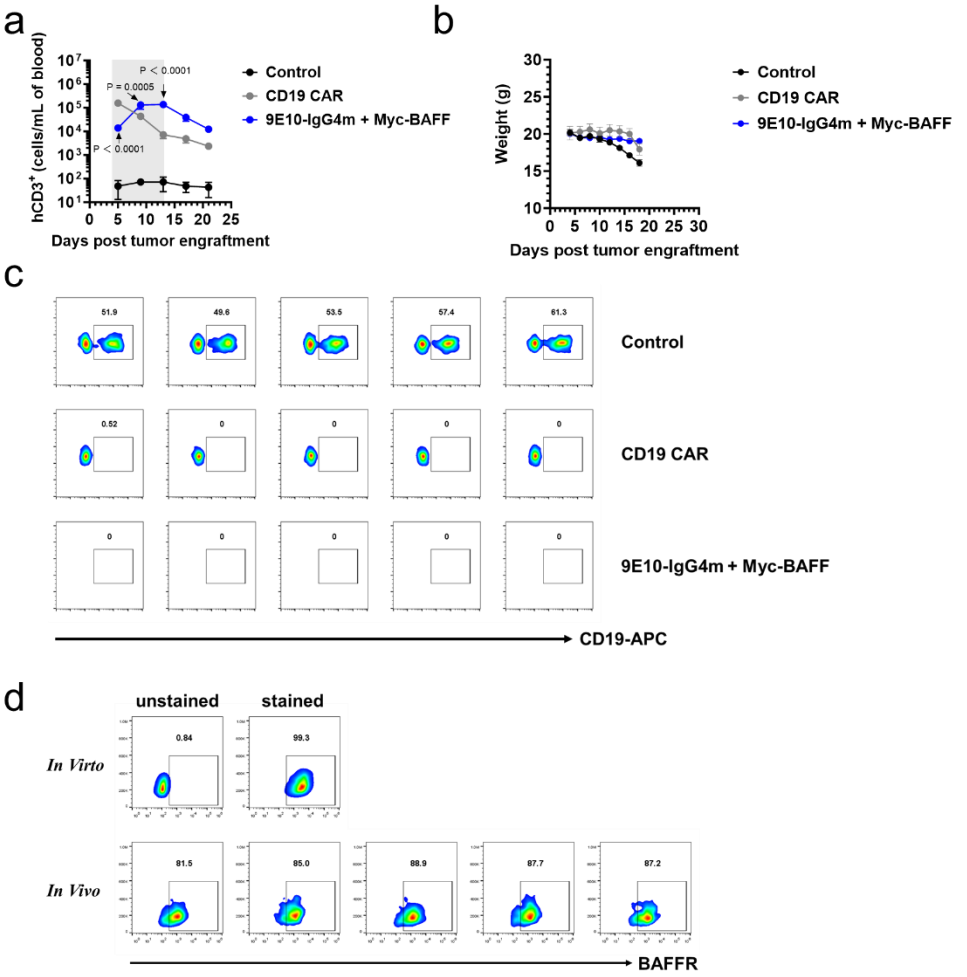

Supplementary Figure 22. *In vivo* persistence, body weight monitoring and tumor cell antigens detection to compare BAFF-based sCAR-T cells and CD19 CAR-T cells in the heterogeneous B-ALL model.

NSG mice (n = 5/group) were i.v. inoculated with a mixture of Nalm6-WT and Nalm6-CD19KO cells (0.5×10^6 cells per mouse at a ratio of 1:1). After infusion of the corresponding CAR-T cells, switches were i.p. administered at a dose of 1 mg/kg daily for a total of ten doses. (a) Assessment of persistent human $CD3^+$ ($hCD3^+$) T cells in peripheral blood by flow cytometry over a 3-week follow-up period. Two-way ANOVA multiple comparisons in Dunnett correction were used to assess significance, comparing 9E10-IgG4m CAR-T (with Myc-BAFF) and CD19 CAR-T at each time point. (b) Mouse body weight was monitored every other day. (c) CD19 expression on the tumor cell surface was analyzed on day 18 of the experiment using flow cytometry. The tumor cells were identified as GFP^+CD19^+ or GFP^+CD19^-. (d) In mice in which tumor relapse was observed after treatment with BAFF-based sCAR-T cells, BAFFR expression on the tumor cell surface was analyzed on day 36. BAFFR expression of Nalm6 cells cultured *in vitro* was used as the flow cytometry gating strategy. N represents biological replicates from different mice. Data in this figure are representative of one of two independent experiments. Error bars represent mean ± SEM. Source data of (a-b) are provided in the Source Data file.

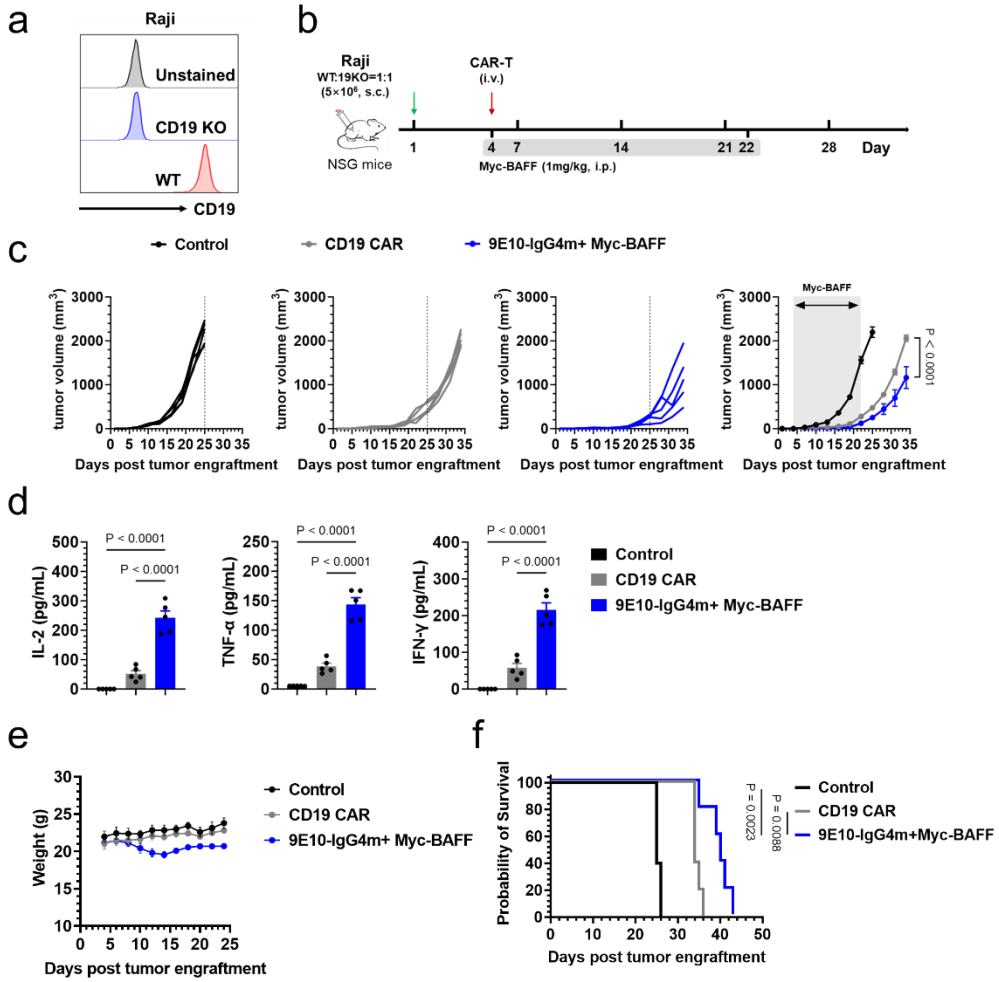

Supplementary Figure 23. *In vivo* efficacy comparison of split-design BAFF-based sCAR-T cells with CD19 CAR-T cells in the heterogeneous NHL model.

(a) Validation of Raji antigen escape variants. (b) Timeline of the *in vivo* experiments. NSG mice (n = 5 mice/group) received s.c. inoculation of a cell mixture of Raji-WT and Raji-CD19KO cells (5×10^6 cells per mouse, at a ratio of 1:1). Three days after tumor engraftment, the mice were i.v. injected with 30×10^6 corresponding CAR-T cells. Switches were i.p. administered at a dose of 1 mg/kg every other day for a total of ten doses. Each group of mice also received i.p. administration of 100 ng of human IL-7 for 10 injections. (c) Tumor volume (mm^3) was monitored over a period of 34 days. It was calculated using the formula (length × $width^2$)/2. Two-way ANOVA multiple comparisons in Dunnett correction were used to assess significance, comparing 9E10-IgG4m CAR-T (with Myc-BAFF) and CD19 CAR-T. (d) Serum inflammatory cytokine levels were assessed by ELISA 24 hours after CAR-T-cell infusion. One-way ANOVA multiple comparisons in Dunnett correction were used to assess significance. (e) Changes in the body weights of the mice during drug administration. (f) Survival curves of mice subjected to the indicated treatments, compared using the log-rank (Mantel–Cox) test. All n represents biological replicates from different mice. Data in this figure are representative of one of two independent experiments. Error bars represent mean ± SEM. Source data are provided in the Source Data file.

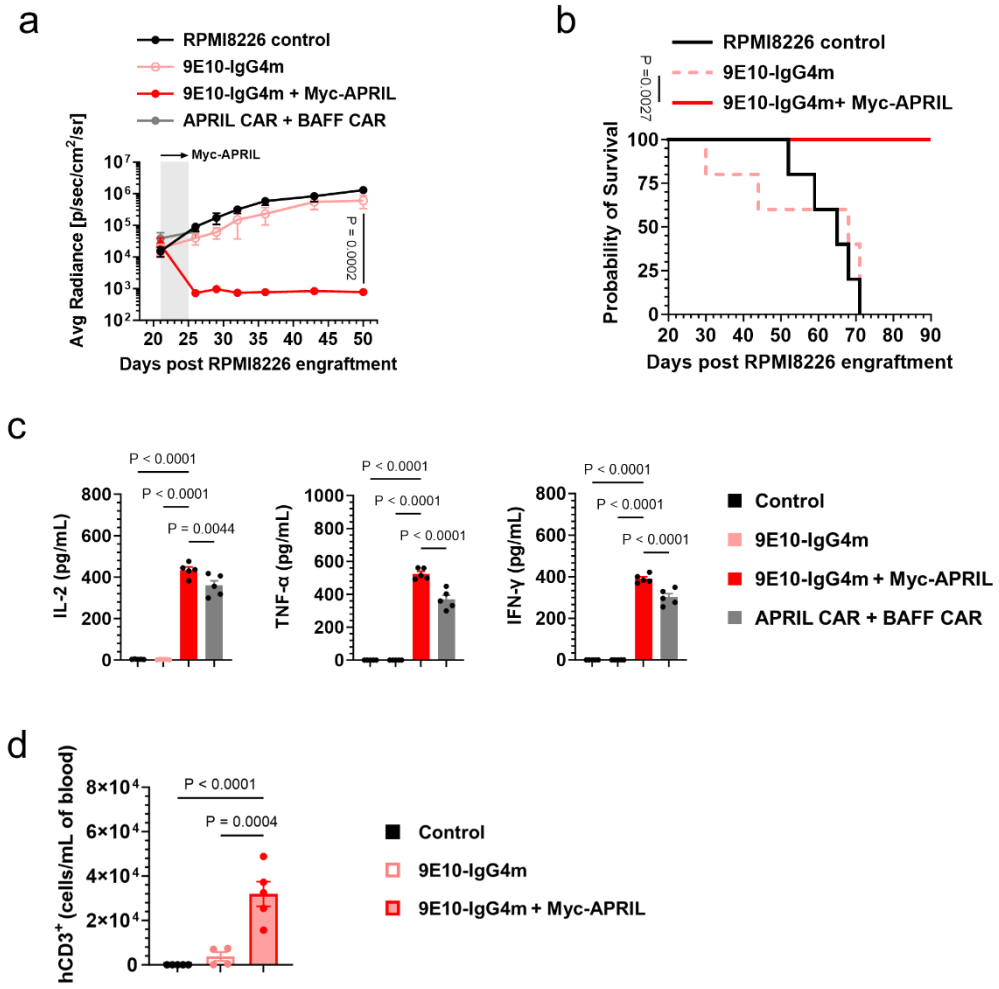

Supplementary Figure 24. Additional data on the *in vivo* synergistic effects of the split-design ligand-based CAR-T-cell system.

(a) Tumor burden of the MM single-tumor model over time, quantified as average radiance (p/s/cm^2/sr) from luminescence. Two-way ANOVA multiple comparisons in Dunnett correction were used to assess significance, comparing 9E10-IgG4m with and without Myc-APRIL. (b) Survival curves of mice subjected to the indicated treatments, compared using the log-rank (Mantel–Cox) test. (c) Serum inflammatory cytokine release was evaluated by ELISA 24 hours after the first dose of Myc-APRIL. One-way ANOVA multiple comparisons in Dunnett correction were used to assess significance. (d) On the 39th day of the experiment, the presence of persistent human CD3$^+$ (hCD3$^+$) engineered CAR-T cells in the peripheral blood was assessed in RPMI8226-bearing mice by flow cytometry. One-way ANOVA multiple comparisons in Dunnett correction were used to assess significance. All n (n = 5/group) represents biological replicates from different mice. Data in this figure are representative of one of two independent experiments. Error bars represent mean ± SEM. Source data are provided in the Source Data file.

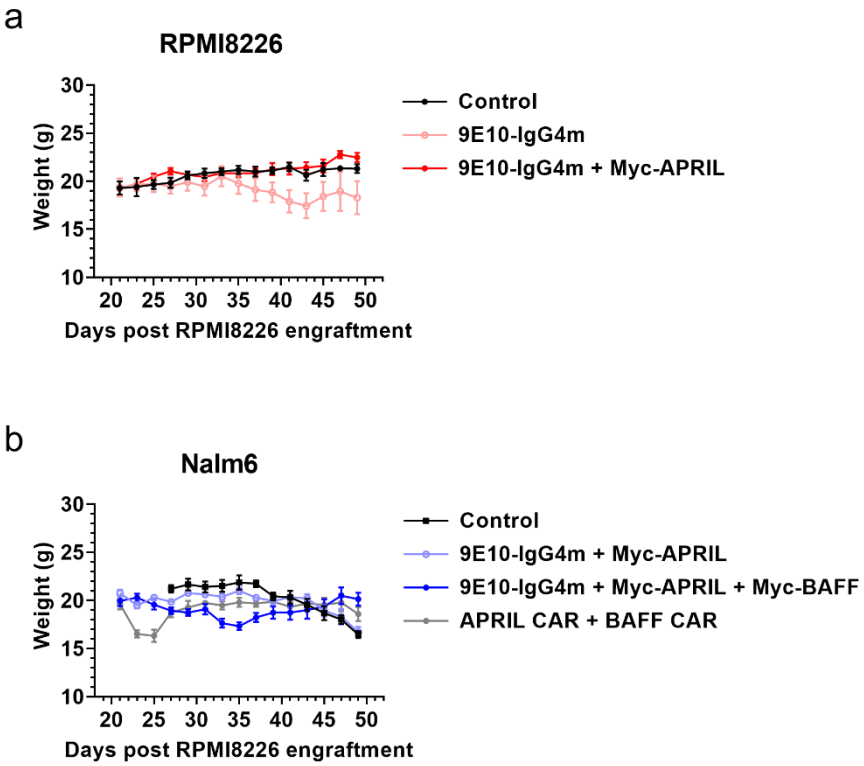

Supplementary Figure 25. Monitoring of mouse body weight in the *in vivo* synergistic model. A dual tumor model (n = 5 mice/group) comprising RPMI8226 and Nalm6 cells was employed to illustrate the *in vivo* synergistic efficacy of 9E10-IgG4m CAR-T cells redirected by APRIL- and BAFF-based switches. (a) Monitoring of mouse body weight in the RPMI8226 single tumor model. (b) Monitoring of mouse body weight in the RPMI8226 and Nalm6 dual tumor model. Body weight was monitored every other day. Error bars represent mean ± SEM. N represents biological replicates from different mice. Data in this figure are representative of one of two independent experiments. Source data are provided in the Source Data file.

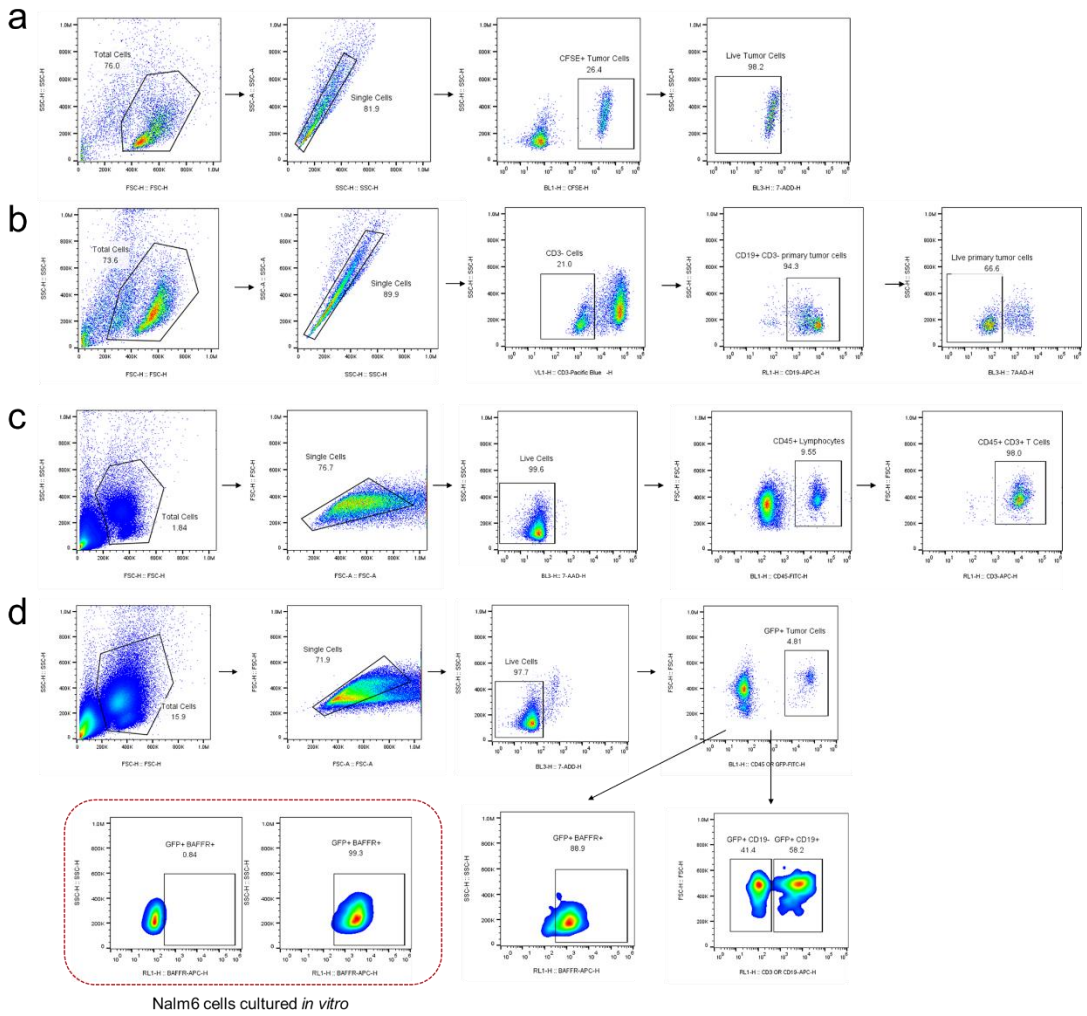

Supplementary Figure 26. Flow cytometry gating strategy.

(a) Representative flow cytometric analysis of the *in vitro* tumor cell line cytotoxicity assay. Remaining live target cells were identified as 7-AAD$^-$CFSE$^+$. (b) Representative flow cytometric analysis of the *in vitro* primary patient tumor cell cytotoxicity assay (Supplementary Figure 10). Remaining live target cells were identified as 7-AAD$^-$CD3$^-$CD19$^+$. (c) Representative flow cytometric analysis of *in vivo* CAR-T cell persistence in peripheral blood (Figure 4l, 6g, Supplementary Figure 22a, 24d). CAR-T cells were identified as 7-AAD$^-$CD45$^+$CD3$^+$. (d) Representative flow cytometric analysis of *in vivo* CD19 or BAFFR antigen expression on the tumor cell surface following CAR-T infusion (Supplementary Figure 22c-d). BAFFR expression in Nalm6 cells cultured *in vitro* served as a baseline for gating. Tumor cells were identified as 7-AAD$^-$GFP$^+$.

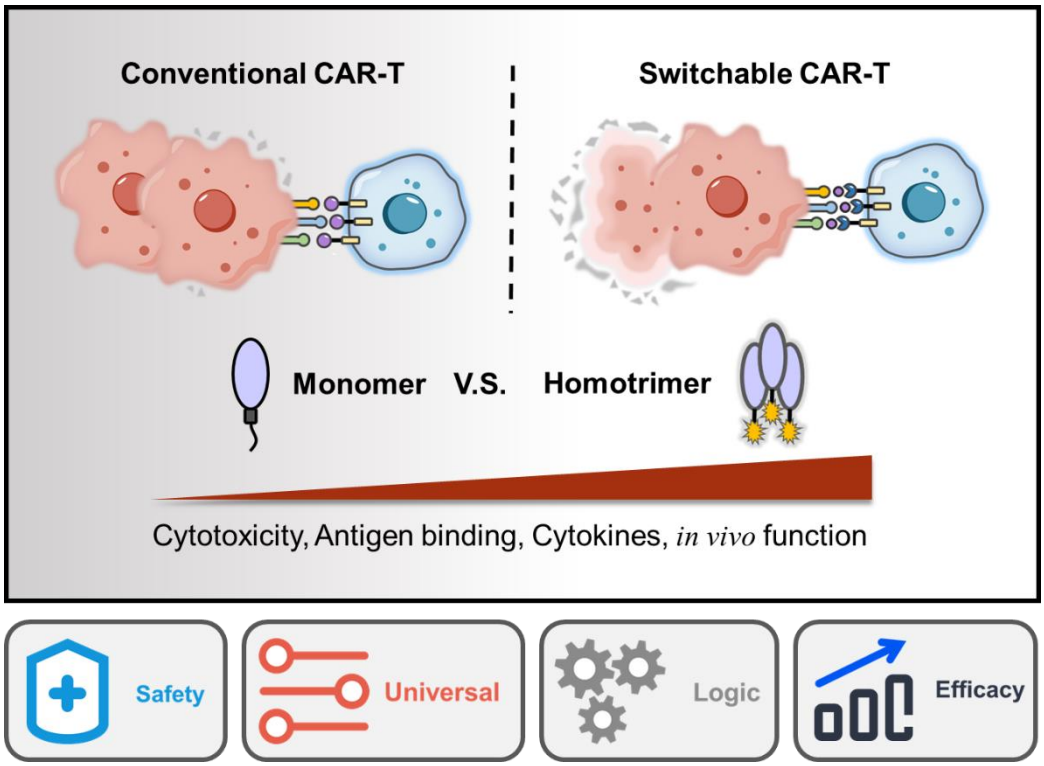

Supplementary Figure 27. A schematic diagram of the design framework for this study. The split-design approach guarantees the optimal target-binding specificity of ligand-based CAR-T cells. APRIL- and BAFF-based sCAR-T cells exhibit enhanced antitumor activity and broadly target various B-cell malignancies.

Supplementary Table 1. Statistical summary of B-cell malignancy cell lines used in the study.

Cell line	Cancer type	BCMA	TACI	BAFFR
Raji	Burkitt's Lymphoma	+	+	+
IM9	Multiple Myeloma	+	+	+
Jeko-1	Mantle Cell Lymphoma	+	+	+
MEC-1	Chronic Lymphocytic Leukemia	+	+	+
RPMI8226	Plasmacytoma	+	+	-
MM.1S	Immunoglobulin A Lambda Myeloma	+	+	-
Nalm6	Acute Lymphoblastic Leukemia	-	+	+
K562	Chronic Myelogenous Leukemia	-	-	-

Supplementary Table 2. Statistical data for retention volume of standard proteins.

Name	MW/Da	Retention/mL
Bovine serum albumin	66000	13.64
Ovalbumin	43000	14.71
Carbonic anhydrase	29000	16.09
Ribonuclease A	13700	17.34
Aprotinin	6500	19.15

Supplementary Table 3. Statistical data for retention volume of APRIL- or BAFF-based switches.

Name	MW/Da	Retention/mL
Myc-BAFF	56000	13.82
BAFF-Myc	56000	13.89
Myc-APRIL	50000	14.47
APRIL-Myc	50000	14.43

Supplementary Table 4. Statistical data for patients with B-cell malignancies.

Patient	Sex	Age, y	Diagnosis
Pt #1	female	42	Ph^+ B-ALL
Pt #2	male	59	MCL/CLL
Pt #3	male	51	SLL/CLL
Pt #4	male	35	MCL
Pt #5	male	50	MM
Pt #6	male	-	MGRS
Pt #7	male	42	MM
Pt #8	male	55	MM
Pt #9	female	63	MM
Pt #10	male	84	MM
Pt #11	male	81	MM

Ph^+ B-ALL, Philadelphia-chromosome positive acute lymphoblastic leukemia; **MCL**, Mantle-cell lymphoma; **SLL**, Small Lymphocytic Lymphoma; **CLL**, Chronic lymphocytic leukemia; **MM**, Multiple myeloma; **MGRS**, monoclonal gammopathy of renal significance.